A TRANSIENT TWO-DIMENTIONAL INVERSE ESTIMATION OF THE METAL-MOLD HEAT TRANSFER COEFFICIENT DURING SQUEEZE CASTING of AL-4.5WT%CU

A.A. Ranjbar*, A. Ghaderi, P. Dousti
Faculty of Mechanical Engineering, Babol University of Technology, Babol, Iran
ranjbar@nit.ac.ir; a.ghaderi@stu.nit.ac.ir; dousti@stu.nit.ac.ir

M. Famouri
Mechanical Engineering Department, University of South Carolina, Columbia, SC, USA
famouri@email.sc.edu

*Corresponding Author

(Received: November 24, 2010 – Accepted: February 10, 2011)

Abstract In this paper, a transient, two-dimensional and nonlinear inverse heat conduction problem in solidification process is considered. Genetic algorithm is applied for the identification of the interfacial heat transfer coefficients during squeeze casting of commercial aluminum alloy (Al-4.5wt%Cu) by assuming a priori information regarding the functional form of the unknown heat transfer coefficients found in open literature. In this work, simulated (noisy and filtered) temperatures are used instead of experimental data. The estimated temperatures are obtained from the direct numerical solution of a two-dimensional conductive model. A modified elitist genetic algorithm is used to minimize the least square objective function containing estimated and simulated temperatures. The accuracy of the proposed method is assessed by comparing the estimated with the pre-selected parameters.

Keywords Inverse Heat Conduction Problem, Parameter Estimation, Genetic Algorithm, Interfacial Heat Transfer Coefficients, Data Filtering

چکیده در این تحقیق مسئله انتقال حرارت هدایتی دو بعدی غیر خطی مورد بررسی قرار گرفته است. الگوریتم ژنتیک برای بدست آوردن ضریب انتقال حرارت مرزی در فرایند انجماد فشاری آلیاژ آلومینیوم (مس 4/5 % وزنی) به کار رفته است، با فرض اینکه اطلاعات اولیه فرم تابع ضریب انتقال حرارت نا معلوم، بر اساس تحقیقات انجام شده در گذشته بدست آمده است. در این تحقیق به جای استفاده از داده‌های آزمایشگاهی از دماهای شبیه سازی (با نویز و فیلتر) استفاده شده است. دماهای تخمینی از حل عددی مستقیم مدل انتقال حرارت هدایتی دو بعدی بدست آمده است. الگوریتم ژنتیک نخبه گرای بهبود یافته برای کمینه سازی تابع حداقل مربعات هدف شامل دماهای تخمینی و شبیه سازی شده به کار گرفته شده است. دقت و کارایی روش پیشنهادی با مقایسه پارامترهای تخمینی بدست آمده و از پیش تعیین شده بررسی شده است.

1. INTRODUCTION

Estimation of boundary conditions at the surface of a heat-conducting body from measured temperature profiles is typically called Inverse Heat Conduction Problem (IHCP). Boundary estimation problems have many applications in various branches of science and engineering when surface temperatures or heat fluxes need to be established in the unreachable areas of the surface from corresponding measurements at reachable areas. Specific examples are the determination of the extremely high thermal loads during atmospheric reentry of a space vehicle [1], the metal quenching process by array of jets [2], grinding process [3, 4], and the heat transfer between the casting and the mould [5].The solution to these inverse problems is not straightforward as the unavoidable noise in the data can produce large or even unbounded deviations in the results. This is due to the "ill posed" nature of the IHCP [6]. IHCP can be efficiently employed when some parameters, such as thermal conductivity or heat flux, are not precisely known. Zhou et al. [7] solved IHCP in a two-dimensional rectangular object by using the

conjugate gradient method (CGM) with temperature and heat flux measured at the boundary opposite to the heated boundary. In general, prediction of solution for the IHCP can be achieved via minimization of sum of squared error function, which is focused on the difference among the values of the measured temperatures and those obtained by an efficient computational method. The unknown thermal coefficients on the mathematical model (i.e., thermal properties, boundary or initial conditions) that dedicate an acceptable value for the aforementioned error function, based on the iterative regularization method, are the solutions of the IHCP. In order to solve the IHCP, there are several methods most noted of which are the sequential function estimation [6], the Tikhonov regularization [8], the conjugate gradient method [9-10], the variable metric method [11] and finally the evolutionary algorithms like Particle Swarm Optimization (PSO) [12] or Genetic Algorithm (GA) [13-17]. The GA and PSO are not, in essence, gradient-based search methods and have recently received the most attention. Not being sensitive to the noise or the number of sensors are the most important features of these method.

Inverse problems are encountered in various branches of science and engineering, because it is very important for the engineers to gain a valuable insight into the comprehension of the evolution of the solidification process to predict correctly and to improve the quality of solidified materials in material processing [18]. As solidification progresses, the mold expands due to the absorption of heat and the solidified metal shrinks during cooling, as a result a gap develops because pressure becomes insufficient to maintain a conforming contact at the interface. This temporally and spatially varying air gap introduces an additional resistance to the heat flow from the metal to the mold. This thermal resistance has a considerable influence on the rate of solidification and thus, affects the microstructure formation [19]. Ranjbar et al. [18] indicated that during the solidification, the Interfacial Heat Transfer Coefficient (IHTC) between the cast and mould is one of the most important factors that influence the solidification process, the soundness of the cast product and the resulted mechanical properties. Squeeze casting is one of the improved casting techniques [20], used for the production of engineering components mostly in non-ferrous metals by the application of pressure on the cast metal to eliminate defects associated with shrinkage cavities and/or gas porosity. By squeeze casting operation, the liquid molten metal is compressed under pressure inside the mould cavity of a re-usable metal mould, usually made of steel (see Fig. 1). The advantages of the squeeze cast products are mainly near-zero gas porosity or shrinkage porosity, better mechanical properties and reduced metal wastage. Researchers have reported that the mechanical properties of a squeeze cast item can be as good as wrought products of similar composition [21-22].

GA is a robust, non-gradient algorithm that belongs to the field of evolutionary algorithms. Garcia [16] developed an excellent GA code to optimize the experiment design for estimation of temperature-dependent thermal properties (TDTPs) of composite materials. Imani et al. [15] and Imani [17] defined a simple one-dimensional model and used temperature history taken from one sensor to simultaneously estimate thermal conductivity and heat capacity based on TDTPs. They used Modified Elitist Genetic Algorithm (MEGA) in order to minimize the Root Mean Square (RMS) resulted by temperature differences between estimated and reference temperatures. Ranjbar et al. [14] extended the former model in two dimensions and tested different forms of functions for thermal conductivity and heat capacity. Loulou et al. [23] experimentally studied and quantified the thermal contact resistance during the first stage of solidification. They claimed that the thermal contact resistance changed in stepwise manner during the first stage of solidification. Lau et al. [24] studied the interfacial heat transfer between an iron casting and a metallic mold. IHTC was found to drop rapidly during the first stage of solidification and then increase with the experimental results. Martorano and Capocchi [25] presented an analysis of heat flow across the metal-mold interface. Adili et al. [26] developed and used genetic algorithm to identify thermophysical properties of fouling deposited onto the internal surface of a heat exchanger. The results of the estimation procedure show on the one hand the efficiency and the stability of the developed genetic algorithm to estimate the

thermophysical properties of fouling and the high accuracy of the obtained results on the other hand. Santos et al. [27] determined IHTC for casting of various compositions of Al-Cu and Sn-Pb alloys. They represented IHTC as an exponential form and time dependent. Famouri [13] investigated on estimation of IHTC at the metal-mould interface in two dimensions during solidification of Sn-Pb alloys. He utilized MEGA to minimize the RMS. Aweda and Adeyemi [28] experimentally estimated IHTC during squeeze casting of Aluminum. He studied effects of applied pressures changes and metal solidification temperatures on the values of the heat transfer coefficients of molten aluminum in squeeze casting operation. Cho and Hong [29] studied heat transfer coefficients at the casting/die interface in squeeze casting and applied a single load (50 MPa) with die heating and concluded that heat transfer coefficient increases with the application of pressure.

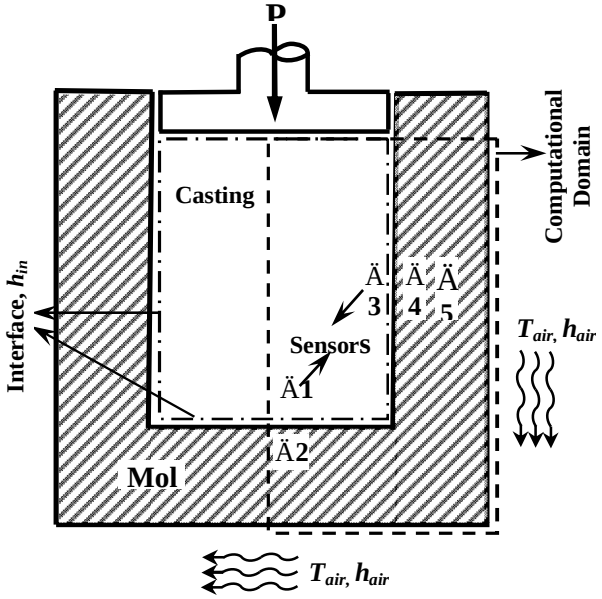

Figure 1. Schematic diagram of squeeze casting, sensor locations, main computational domain, interfaces and the connection with outside.

There are some published information on the study of the IHTC between cast and mould during the squeeze casting, as given above, but there is no published work yet on estimation of IHTC for molten aluminum in squeeze casting operation by evolutionary algorithm such as GA. The aim of the present work is to estimate IHTC based on MEGA. Present model is non-linear case and there is no analytical solution for this model. In this study, 5 sensors are used for temperature history and also the defined model is a two-dimensional practical one with appropriate boundary conditions. Finite Difference Method (FDM) is used as the direct solution to obtain both simulated and estimated temperature based on pre-selected and estimated IHTC, respectively.

2. MATHEMATICAL MODEL

The two-dimensional schematic view of problem is shown in Fig. 1. Interfaces and main computational domain are clearly defined in the figure. The whole computational domain is divided into three computational domains each of which has its own boundary conditions, initial conditions and origin as illustrated in Fig. 2. Implementing these boundary conditions at interfaces between the mold and the cast in convective terms is brought about the IHTC which are unknown. As the effects of fluid flow in the liquid phase are negligible, the convective heat transfer is neglected within the domains and therefore, the phase-change problem is formulated only in terms of heat conduction [9]. The governing equations and the boundary conditions for each computational domain - which are shown in the Fig. 2 - are as following:

Computational domain 1 (Cast):

$$\frac{\partial^2 T_C}{\partial x^2}+\frac{\partial^2 T_C}{\partial y^2}=\left(\frac{r_C}{K_C}\right)\frac{\partial H_C}{\partial t} \qquad t>0 \qquad (1)$$

$$T_C = T_{\text{initial}} \qquad t=0 \qquad (2)$$

$$K_c\left(\frac{\partial T_C}{\partial y}\right)_{y=0} = h_{in1}(t)\left(T_C - T_M\Big|_{y=Ly2}^{Domain\,2}\right) \qquad y=0 \qquad (3)$$

$$\left(\frac{\partial T_C}{\partial y}\right)_{y=Ly1} = 0 \qquad y=L_{y1} \qquad (4)$$

$$\left(\frac{\partial T_C}{\partial x}\right)_{x=0} = 0 \qquad x=0 \qquad (5)$$

$$\left(\frac{\partial T_C}{\partial x}\right)_{x=Lx1} = h_{in2}(t)\left(T_C - T_M\big|_{x=0}^{Domain3}\right) \quad x = L_{x1} \qquad (6)$$

Computational domain 2 (Mold):

$$\frac{\partial^2 T_M}{\partial x^2} + \frac{\partial^2 T_M}{\partial y^2} = \left(\frac{r_M C_{pM}}{K_M}\right)\frac{\partial T_M}{\partial t} \qquad t > 0 \qquad (7)$$

$$T_M = T_{\text{air}} \qquad t = 0 \qquad (8)$$

$$K_M\left(\frac{\partial T_M}{\partial y}\right)_{y=0} = h_{air}(T_M - T_{air}) \qquad y = 0 \qquad (9)$$

$$K_M\left(\frac{\partial T_M}{\partial y}\right)_{y=Ly2} = -h_{in1}(t)\left(T_M - T_C\big|_{y=0}^{Domain1}\right) \qquad y = L_{y2} \qquad (10)$$

$$\left(\frac{\partial T_M}{\partial x}\right)_{x=0} = 0 \qquad x = 0 \qquad (11)$$

$$\left(\frac{\partial T_M}{\partial x}\right)_{x=Lx2} = \left(\frac{\partial T_M}{\partial x}\right)_{x=0}^{Domain3} \qquad x = L_{x2} \qquad (12)$$

Computational domain 3 (Mold):

$$\frac{\partial^2 T_M}{\partial x^2} + \frac{\partial^2 T_M}{\partial y^2} = \left(\frac{r_M C_{pM}}{K_M}\right)\frac{\partial T_M}{\partial t} \qquad t > 0 \qquad (13)$$

$$T_M = T_{\text{air}} \qquad t = 0 \qquad (14)$$

$$K_M\left(\frac{\partial T_M}{\partial y}\right)_{y=0} = h_{air}(T_M - T_{air}) \qquad y = 0 \qquad (15)$$

$$\left(\partial T_M / \partial y\right)\big|_{y=Ly3} = 0 \qquad y = L_{y3} \qquad (16)$$

$$\begin{cases} K_M\left(\dfrac{\partial T_M}{\partial x}\right)_{x=0} = h_{in2}(t)\left(T_M - T_C\big|_{x=Lx1}^{Domain1}\right), y > Ly2 \\ K_M\left(\dfrac{\partial T_M}{\partial x}\right)_{x=0} = K_M\left(\dfrac{\partial T_M}{\partial x}\right)_{x=Lx2}^{Domain2}, y \le Ly2 \end{cases} \qquad x = 0 \qquad (17)$$

$$K_M\left(\frac{\partial T_M}{\partial x}\right)_{x=Lx3} = -h_{air}(T_M - T_{air}) \qquad x = L_{x3} \qquad (18)$$

where K, ρ, C_p, T, h, H, t are the thermal conductivity, density, specific heat, temperature, heat transfer coefficient, enthalpy and time, respectively. Subscripts M and C refer to mold and cast respectively. The $h_{in2}(t)$, $h_{in1}(t)$ and $h_{air}(t)$ are the heat transfer coefficients between the mold and cast (side and bottom surfaces of cast, respectively) and heat transfer coefficients between the mold and the environment. The change in the enthalpy of the casting material is considered as $dH_c = C_{pC}\,dT$.

The phase changing problem (Eq. (1)) during solidification was handled by the enthalpy method [30]. This equation subjects to the boundary and initial conditions along with other equations, are solved by Crank-Nicholson technique. In this study, T_{init} and T_{air} are considered as 993 and 296 K. Steel AISI304 is selected as the mold. The cast, metallic mold materials and their thermo-physical properties used in this simulation are summarized in Table 1 and some of them could be found in Garcia et al. [31].

In this study, the unknown IHTCs are considered time dependent based on open literature [21, 23, 28, 32] and in the exponential form [18].

$$h_{in1}(t) = p_1 t^{P_2} \qquad (19)$$

$$h_{in2}(t) = p_3 t^{P_4} \qquad (20)$$

P_1 to P_4 are unknown parameters.

3. MESUREMENT SIMULATION

In order to simulate the experiment, we use the temperature histories taken from the sensors and denoted them by $Y_{im}(t_i, Sensor_m) \equiv Y_{im}$, $i=1$ to I and $m=1$ to M, where I denotes the number of the time readings and M is the number of sensors. We used 5 sensors in this study ($I=5$). The sensor locations have been shown in Fig. 1 and also all the exact position of each sensor is clear in Table 2 for all the individuals. The measured temperature data, Y_{im}, used in the present inverse

analysis can be determined from the exact temperature solution of the direct solidification problem with the given P_1 to P_4, T_{exact}. Owing to experimental uncertainty, Y_{im} contains the measurement error. Thus, T_{exact} should be modified by Gaussian additive noise in order to simulate experimental measurements. With respect to the eight statistical assumptions in references [6, 9], Y_{im} can be expressed as:

$$Y_{im} = T_{exact}(t_i, Sensor_m) + es \quad (21)$$

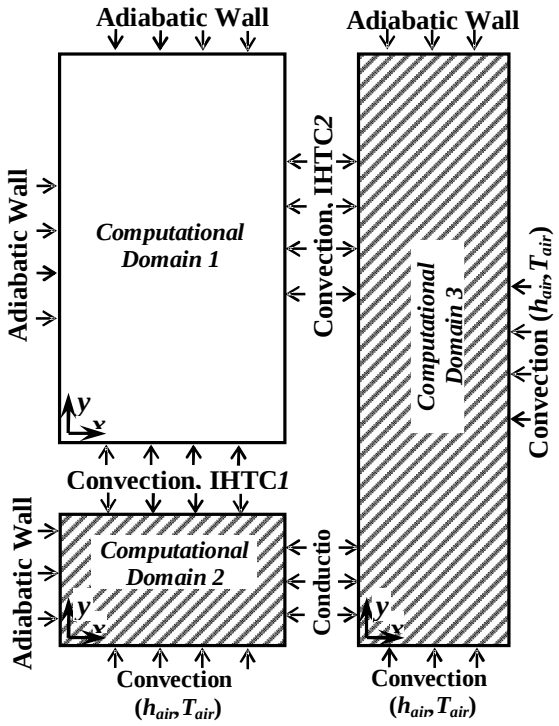

Figure 2. The computational domains with their boundary conditions and connections

TABLE 1. Material thermo-physical properties

Steel AISI304	K (W/m K)		C_p (J /kg K)		ρ (kg/m^3)	
	22.6		582		7900	
Al-4.5wt%Cu	K_S	K_L	C_{pS}	C_{pL}	ρ_S	ρ_L
	193	89	1092	1059	2654	2488
	T_s (K)		T_L (K)		H (J/kg)	
	821		921		381773	

Where s the standard deviation of the temperature measurements and ε is a random variable ranging from -2.576 to 2.576 for normally distributed errors with zero mean and 99% confidence bounds. The product of εs represents the temperature measurement error.

TABLE 2. Exact sensors positions and the domains' dimensions (indices 1, 2 and 3 stand for computational domains 1 to 3, respectively)

Domains	X-Length (mm)	Y-Length (mm)
1	$Lx_1=26$	$Ly_1=76$
2	$Lx_2=26$	$Ly_2=36$
3	$Lx_3=36$	$Ly_3=112$
Sensors	X-Position (mm)	Y-Position (mm)
1	$x_1=2$	$y_1=2$
2	$x_2=2$	$y_2=34$
3	$x_1=24$	$y_1=38$
4	$x_3=2$	$y_3=74$
5	$x_3=4$	$y_3=74$

4. INVERSE HEAT CONDUCTION

The solution of the inverse phase-change problem involving the estimation of metal-mold interfacial heat transfer coefficient is presented here. Inverse parameter estimation methods are based on the minimization of an objective function containing both estimated and measured temperatures [15]. Ordinary Least Squares (OLS) estimator is the far most frequently used method for the parameter estimation as no prior knowledge is needed [33]. OLS estimator was considered in this research. The associated objective function, the least squares error, S, is expressed by:

$$S(b) = \sum_{m=1}^{M}\sum_{i=1}^{I}\left[Y_{im} - T_{im}(b)\right]^2 \quad (22)$$

Where β is the estimated parameter vector containing the unknown parameters; $\hat{Y}_{im}$ is the i^{th}

observation from the m^{th} sensor; M and I are the number of sensors and observations, respectively. $T_{im}(\beta)$ is the calculated temperature from the mathematical model governing (direct solution) the heat transfer phenomena with respect to the estimated parameter vector.

In using equation (22), the IHTCs are found by minimizing the sum of squared differences between the measured and calculated data. The minimization of equation (22) could conceivably be performed by any optimization technique. However, parameter estimation has generally been performed with only a few methods. The use of one method over another is often specific to a certain field of study. The approach investigated in the present work involves the use of a robust non-gradient method, namely the GA method, in the minimization procedure. The motivation for using GAs was to circumvent difficulties of non-convergence in cases when the parameters are correlated or nearly so.

5. GENETIC ALGORITHM

GAs were developed by Goldberg [34]. The common feature of these algorithms is to simulate the search process of natural evolution and take advantage of the Darwinian survival-of-the-fittest principle. The more details about the GA used in present study could be found in these references [13-15, 17]. In short, an individual is a possible solution of an optimization problem with the objective function $S(\beta)$, which is a scalar-valued function of an n-dimensional vector β. The vector β consists of n unknown parameters β_j, with $j=1$ to n. The goodness of each individual is evaluated by a fitness function that is defined from the objective function of the optimization problem. To define a fitness function for minimization problems such as equation (22), it is necessary to change the objective function, because GA works according to the principle of the maximization of the fitness function, and so the fitness function of equation (22) is defined as:

$$f(b)=\frac{1}{.001+\sqrt{S(b)}} \tag{23}$$

The square root function is included to moderate the selection pressure of the GA, and 0.001 is added arbitrarily to limit the maximum of the fitness function and avoid the infinity. The present mechanism to select parents is the combination of Roulette Wheel Selection (RWS) and Tournament selection [35-36]. The modified elitist genetic algorithm started by a successive random search for elite individuals in which only the some first-ranked individual of each initial population is kept for an elite initial population. To do so, instead of N_s individuals, N_N*N_s individuals have been randomized and N_s individuals would be selected out of the whole. A compression factor r_c is then applied in some generations to reduce the parameters' search space as follow:

$$\begin{aligned} U_i\big|_{new} &= (1-r_c)c_{best,i} + r_c\, U_i\big|_{old} \\ L_i\big|_{new} &= (1-r_c)c_{best,i} + r_c\, L_i\big|_{old} \end{aligned} \tag{24}$$

There are many advantages of applying GAs to estimation problems. GAs are easily programmed. Their major strength is that they are derivative-free calculations and, as shown in this work, they do not need any initial guesses. Design of robust GAs is highly application-specific and their performance is difficult to predict. Another significant drawback is the high CPU cost. A mathematical function called $f6$ - as used in previous works [13, 15], was optimized to illustrate the performance of the MEGA. The expression of this function is:

$$f6(x,y)=.5-\frac{\left[\sin\sqrt{x^2+y^2}\right]^2-.5}{\left[1.0+0.01\times\left(x^2+y^2\right)\right]^2} \tag{25}$$

The goal is to optimize $f6$, e.g., to find values of x and y that produce the greatest possible value for $f6$. This function has some interesting features such as a single global optimum, which is $f6(x=0, y=0) = 1$, strong oscillations, and a tiny fraction of the total area for the global regions. Fig. 3 shows a typical increase of both the fitness (function $f6$) of the best individual and the average fitness of the population obtained from MEGA for different runs.

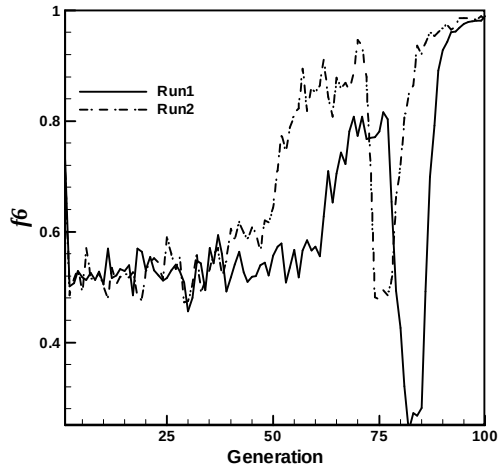

(a)

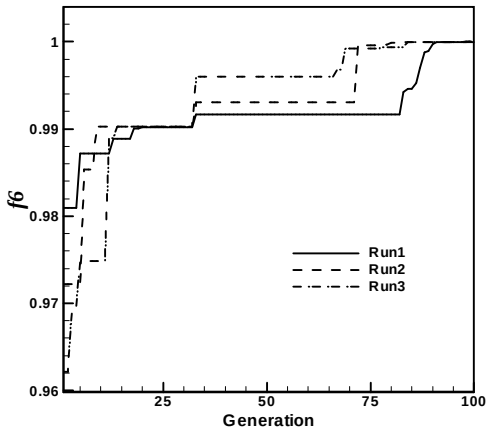

(b)

Figure 3. Evolution of fitness function f_6 for different runs (a) Average, (b) Best

Accuracy of the present algorithm has been shown in Table 3. Present algorithm successfully finds the global optimum just with 100 generations whereby *x* and *y* errors are of (-4) to (-7) order.

6. METHODOLOGY

A flowchart of the proposed method for IHTCs estimation is shown in Fig. 4. A simulated experiment was performed with adding Gaussian white noise to the exact solution of the direct conductive model. To simulate the experiment, the pre-selected IHTCs are assumed for a case of dependency as:

$$h_{in}(t) = p_1 t^{P_2} = 4050t^{-0.2291} \quad (26)$$

$$h_{in2}(t) = p_3 t^{P_4} = 4332t^{-0.2359} \quad (27)$$

A total of 1000 simulated measurements containing additive, uncorrelated, and normally distributed errors with zero mean and constant standard deviation of $s = 0.01T_{max}$ were assumed available for the estimation procedure, where T_{max} is the maximum of the exact temperature in the simulated experiment. Measurement interval is chosen as 1.5 *s* and the T_{max} is considered as 723 C^o.

Exact simulated temperature measurements for all sensors locations are presented in Fig. 5-(a). Actual measured data could be used for the inverse analysis as illustrated in Fig. 4. A three-point moving average filter is applied to reduce measurement errors. After data filtering, these measurements are used in MEGA to estimate the unknown IHTCs. Filtered temperatures for sensor No.2 and 3 are compared with noisy and exact measurements in Fig. 5-(c and d). It's clear in Fig. 5-(c and d) that the data filtering reduces the noises; this point is obviously shown in Fig. 5-(b).

TABLE 3. The average and best fitness function along with their own best *x, y* resulted by MEGA in different runs for f6

Run	x	y	Best FF	Ave FF
1	3.82082E-05	-6.60195E-05	0.99999999	0.996737
2	1.32018E-04	4.47859E-05	0.99999998	0.997916
3	2.37890E-05	5.86463E-05	1.00000000	0.995085
4	-8.00218E-06	-1.36935E-07	1.00000000	0.997317
5	6.72596E-05	4.12371E-05	0.99999999	0.996445
GA Parameters	NS= 100	PM= 0.1	Search Domain	PR= 0.95
	NG= 100	RC= 0.95	[-50,50]	NN= 40

7. RESULS AND DISCUSSION

Genetic parameters could affect the convergence and performance of the MEGA. There are unfortunately few heuristics to guide a user in the selection of appropriate operators and genetic parameter settings for a particular problem. What can be grasped، from the literature is that good GA performance requires the choice of a moderate population size, a high crossover probability, and a low mutation probability [15]. So, genetic parameters in the current research are chosen as: N_S=100; N_G=1000; P_c=0.99; P_m=0.1; P_r=0.95; r_c=0.99 for 4 unknown parameters (N_P=4). The valid ranges for the unknown parameters are specified to begin the MEGA search, e.g., $P_1, P_3 \in$ [100, 10000] and $P_2, P_4 \in$ [0, -1].

In this work, it is assumed that the form of the estimated IHTCs is priori unknown as in most real-world engineering applications. One may choose different forms of the unknown estimated IHTCs and calculate the RMS error between simulated and estimated temperatures to find minimum RMS error (maximum fitness function). In order to find exponential form of IHTCs, the problem is to find the best combination of parameters (P_1, P_2, P_3 and P_4) to achieve the maximum value of fitness function (minimum of RMS); therefore GA find the best combination of parameters as β vector ($\beta \equiv [P_1, P_2, P_3, P_4]$) to gain the $f(\beta)$ maximum.

The inverse estimation of IHTCs is first performed by assuming exact measurements. Then, analysis is repeated for the noisy measurements with $\sigma=0.01T_{max}$. As randomness plays an important role in each run of the MEGA (two runs with different random seeds will generally produce different output). Figure 6 shows the differences between exact ($\sigma=0$) and noisy ($\sigma=0.01T_{max}$) measurements regarding the fitness function. Fitness functions for both cases are shown in the figures when one of the parameters varies around the pre-selected value of the parameter (e.g. $\beta_1 \in P_1 \pm 0.05 \times P_1$, Fig. 6-(a)) and the others parameters hold exactly the pre-selected value from the exponential estimation (Eq. (26-27)) (e.g. $\beta_i = p_i$). Actually, β_1 stays on the x-axis and vary from $\beta_1 = (1-0.05) \times P_1$ to $\beta_1 = (1+0.05) \times P_1$ and it's the difference between the cases in Fig. 6 and the best fitness sit on the y-axis. In order to make it clear, it should be mentioned that $\beta_2 \equiv P_2 \pm 0.05 \times P_2$, $\beta_3 \equiv P_3 \pm 0.05 \times P_3$ and $\beta_4 \equiv P_4 \pm 0.05 \times P_4$ correspond Fig. 6 (b, c, and d), respectively. Moreover, each figure has one solid and three Dashed-Dot lines. The solid one corresponds to the σ=0 case while the Dashed-Dot lines are from different runs (random temperature error measurements) with $s=0.01T_{max}$. As demonstrated in the legend the solid line corresponds to the left hand y-axis and the other Dashed-Dot lines correspond to the right hand y-axis.

Generally speaking, for the exact measurements case, fitness functions reach the maximum value (1000) as result of negligible error between the exact measurements and direct solution. But for the noisy measurements, fitness functions don't exceed 0.008 due to noises at simulated temperature. Another point came from Fig. 6 is that the optimum parameter to achieve the maximum fitness function value, doesn't exactly fit on the pre-selected value and the optimum point changes a little in different runs due to noisy random temperature. The curves slip and differential range of fitness functions show the satisfactory sensitivity of each parameter.

Based on exact measurements three different runs are presented in Table 4. We have started with exact simulated measurements and tried to find the best parameters ($\beta \equiv [P_1, P_2, P_3, P_4]$). The best and average fitness functions for the runs listed in Table 4 are also shown in figure 7-(a). In the exact measurements case, as it mentioned, due to negligible error between the exact measurements and estimated temperatures, we can access to value 1000 of fitness function that it is clearly shown in Fig. 7(a).

The results obtained from the exact measurements (σ=0) (Table 4) show an excellent agreement between estimated and pre-selected IHTCs. As we can see, the RMS error between simulated and estimated temperatures is very small. For noisy measurement ($s=0.01T_{max}$), 5 different runs have been done and the results are shown in Table 5 and Fig. 7-(b). The good agreement has been observed between the estimated and pre-selected

parameter as well. The best and average fitness functions for noisy measurement have been shown in Fig. 7-(b).
As for this case, due to the noise, the results are a bit different from the pre-selected parameters and also for different runs. As shown in the Table 5, in terms of Relative Error (R.E.), the estimated parameters have an acceptable error. Moreover, the mean estimated parameters have an excellent agreement with the pre-selected parameters. Also in the Fig. 8, the error between mean estimated and pre-selected parameters have been shown in terms of both IHTC and temperature.

TABLE 4. The best fitness and estimated parameters resulted by MEGA for different runs based on exact measurements (σ=0) which are shown in figure 7-(a)

Run	P_1 (4050)	P_2 (-0.2291)	P_3 (4332)	P_4 (-0.2359)	Fitness Function	RMS Error
1	4049.99936	-0.22909996	4332.00065	-0.23590003	905.86	1.08E-08
2	4049.99978	-0.22909998	4331.99994	-0.23589999	976.58	5.75E-10
3	4049.99991	-0.22909999	4331.99993	-0.23589999	986.38	1.90e-10

TABLE 5. The best fitness function and estimated parameters different runs resulted by MEGA based on noisy measurements ($\sigma=0.01T_{max}$)

Run	P_1 (4050)	R.E. (%)	P_2 (-0.2291)	R.E. (%)	P_3 (4332)	R.E. (%)	P_4 (-0.2359)	R.E. (%)	Fitness Function
1	4048.8	0.03	-0.23070	0.70	4347.4	0.35	-0.23670	0.34	7.17E-03
2	4025.4	0.61	-0.22704	0.90	4395.3	1.46	-0.23926	1.43	6.80E-03
3	4068.3	0.45	-0.22930	0.09	4264.4	1.56	-0.23343	1.05	6.84E-03
4	4021.6	0.70	-0.22648	1.15	4325.4	0.15	-0.23532	0.25	6.91E-03
5	4018.1	0.79	-0.22912	0.01	4306.2	0.60	-0.23534	0.24	7.16E-03
Mean	4036.4	0.34	-0.22853	0.25	4327.7	0.10	-0.23601	0.05	

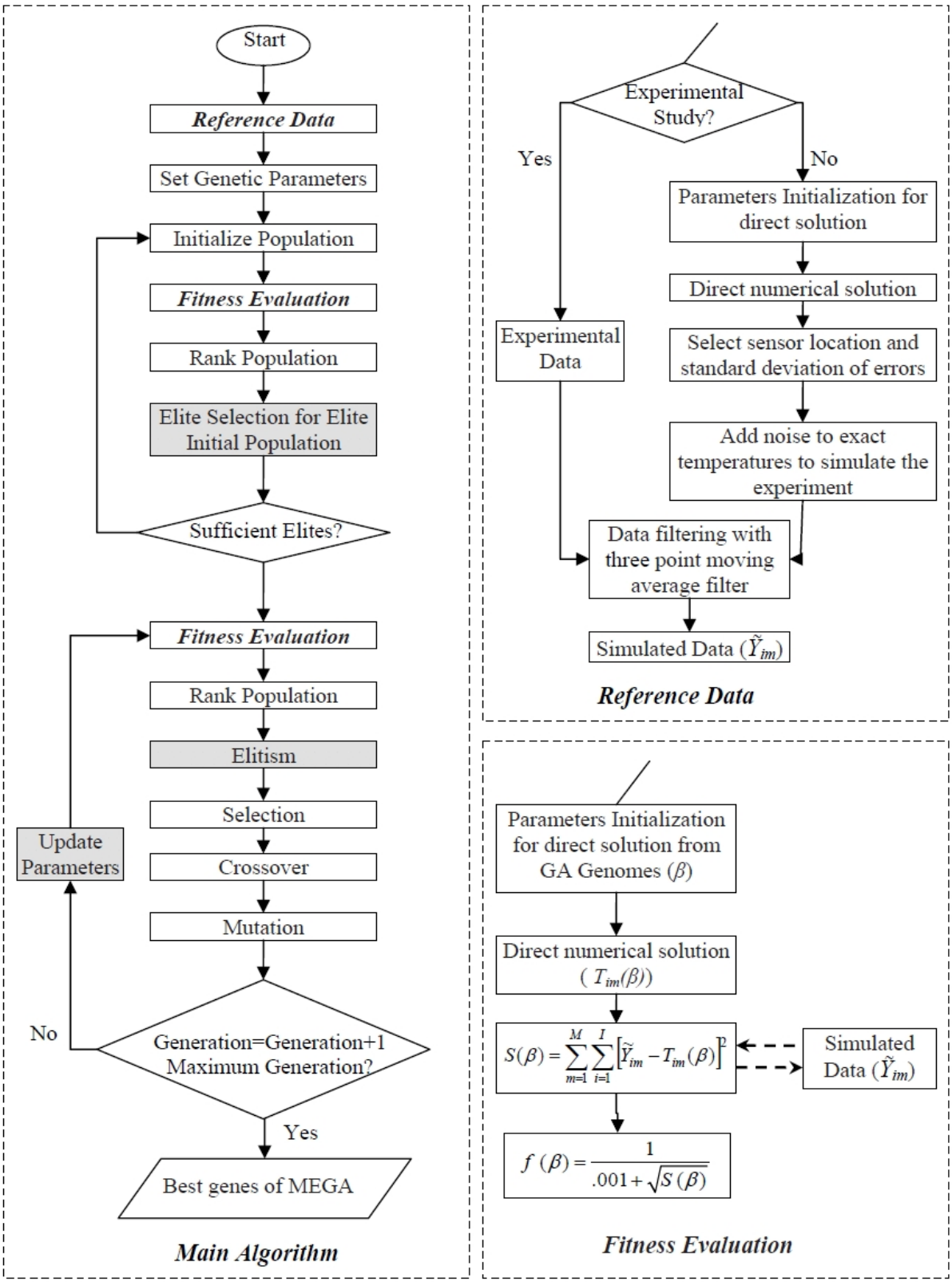

Figure 4. Flowchart of the proposed method

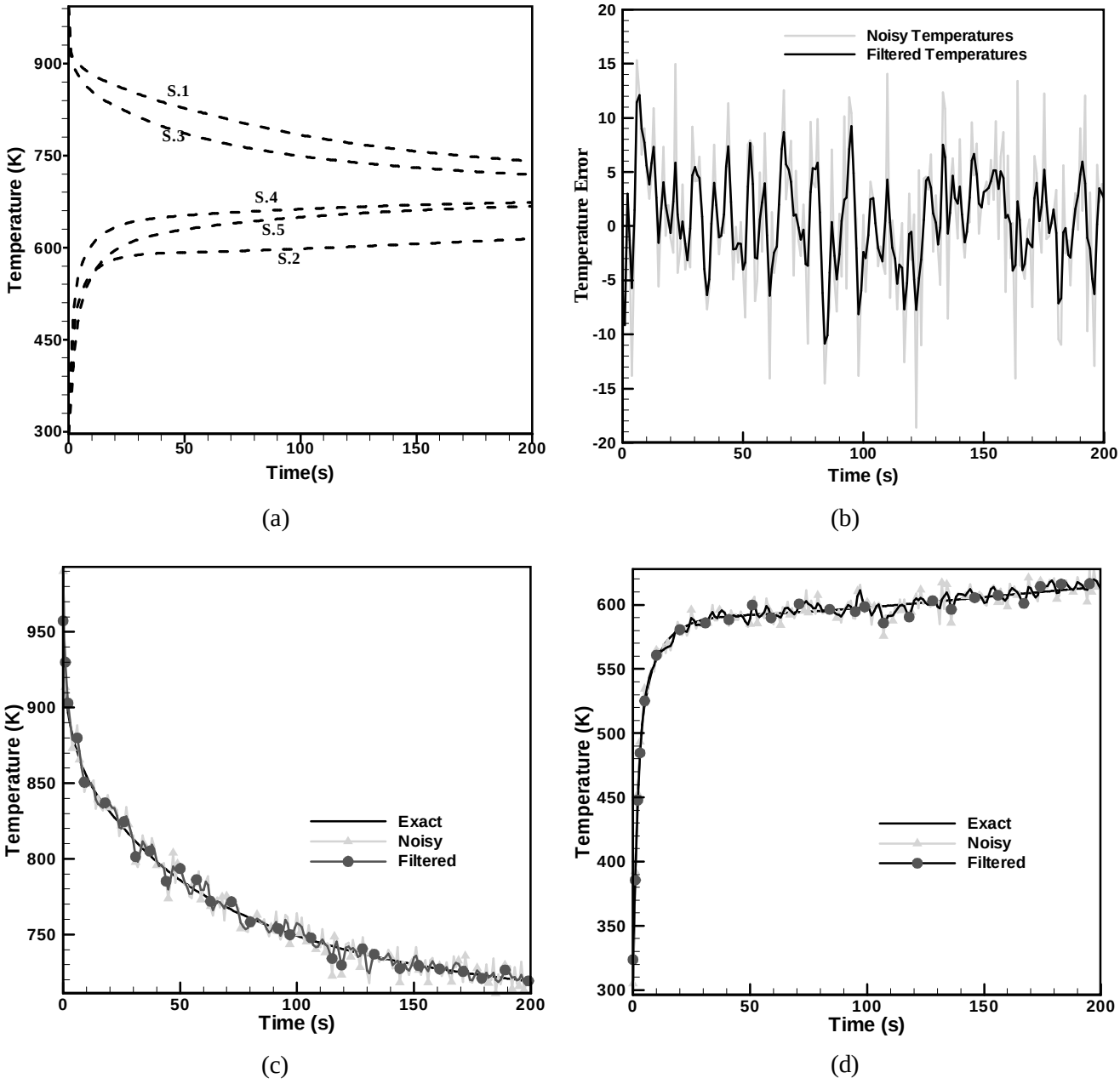

Figure 5. Exact simulated measurements of temperature for sensors No. 1 to 5 (b) Error comparison between noisy and filtered temperature based on exact temperature of sensor No. 5 (c-d) Exact, noisy and filtered temperatures with $s=0.01T_{max}$ for sensor No. 3 and 2

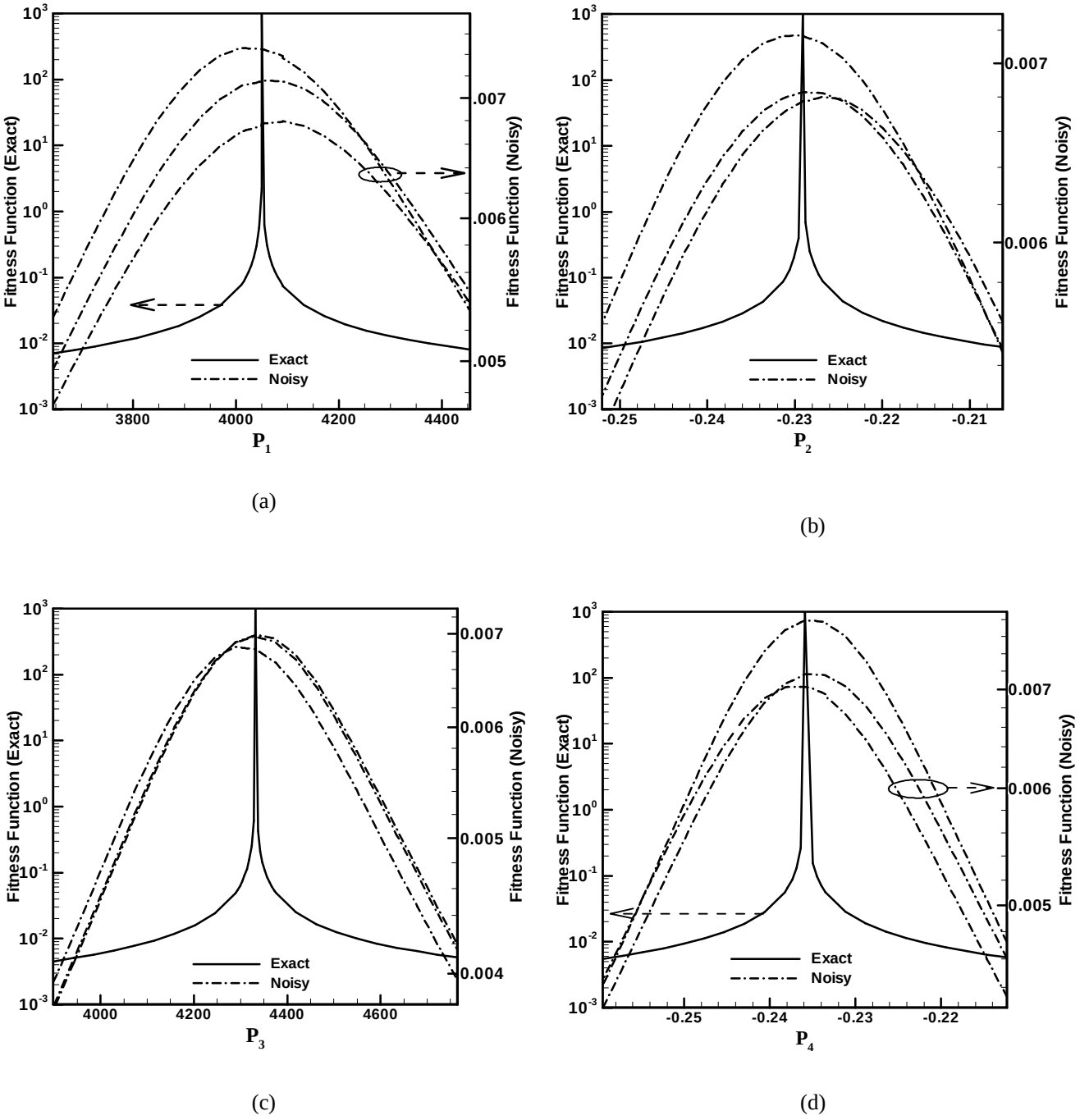

Figure 6. Variation of Fitness Functions versus estimated parameter for Exact ($s=0$) and Noisy ($s=0.01T_{max}$) measurements for different runs, (a) $f(\beta_1 \equiv P_1)$,(b) $f(\beta_2 \equiv P_2)$, (c) $f(\beta_3 \equiv P_3)$ and (d) $f(\beta_4 \equiv P_4)$

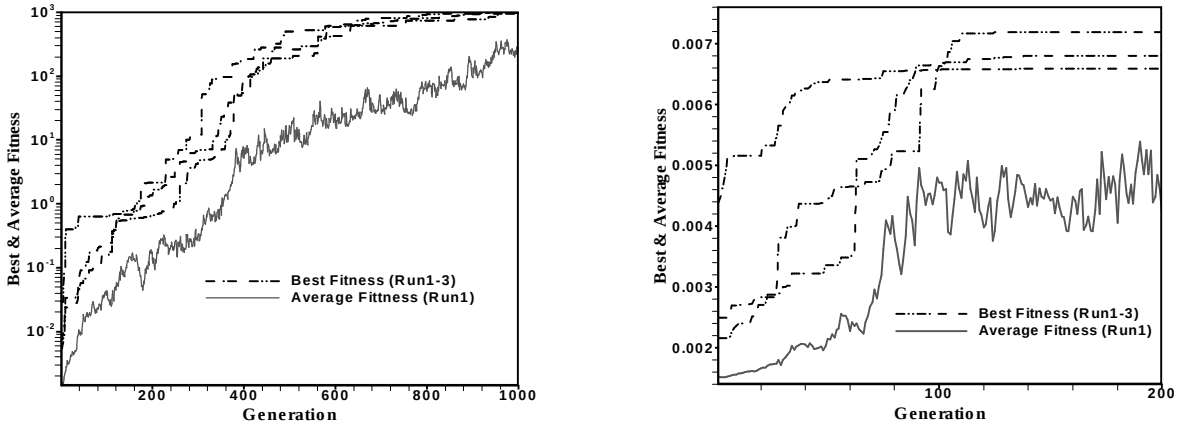

(a) (b)

Figure 7. The best and average fitness functions versus the generations (a) Based on the exact measurements ($s=0$) (b) Based on the noisy measurement ($s=0.01T_{max}$).

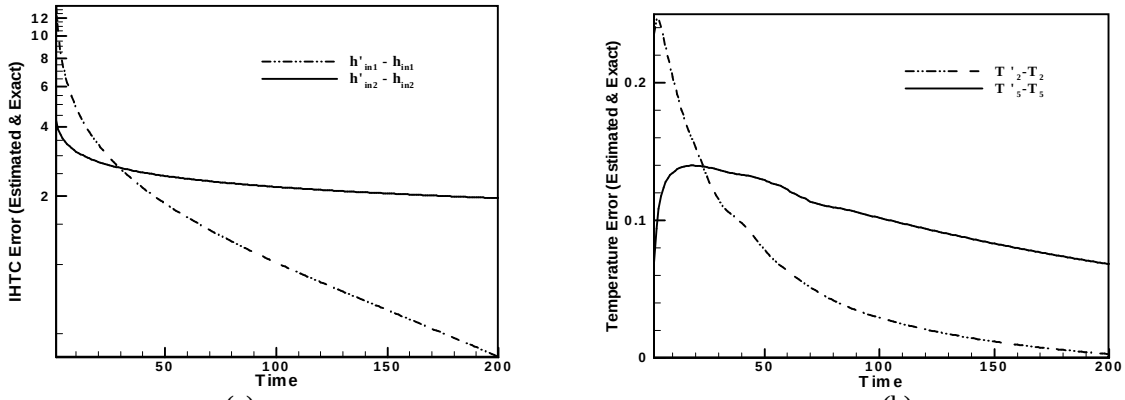

(a) (b)

Figure 8. (a) Comparison of estimated and exact IHTC for both interfaces (h_{in1} and h_{in2}) (b) Comparison of estimated and exact temperature for sensors No. 2 and 5 (prime stands for estimated values)

8. CONCLUTION

A two-dimensional IHCP is solved successfully by MEGA to estimate IHTCs. This estimation is performed for squeeze casting of Aluminum alloy and IHTCs have been estimated at Cast-Mold interfaces. Measurements are taken from sensors. The results show that the measurement errors do not considerably affect the accuracy of the estimates. The proposed method provides a practical and confident prediction in estimating the IHTC. This method is also applicable to other kinds of inverse heat transfer problems such as estimation of the directional thermo-physical properties, unknown heat flux estimation, inverse heat convection, and radiation problems.

9. REFERENCES

1. Hakkaki-Fard, A. and Kowsary, F., "Heat Flux Estimation in a Charring Ablator". ***J. Numer. Heat. Trans.***, Part A, Vol. 53, (2008), 543–560.
2. Nallathambi, A.K. and Specht, E., "Estimation of heat flux in array of jets quenching using experimental and inverse finite element method", ***J. Mater. Process. Technol.***, Vol. 209, (2009), 5325-5332.
3. Honga, K.K. and Lo, C.Y., " An inverse analysis for the heat conduction during a grinding process", ***J. Mater. Process. Technol.***, Vol. 105(1-2), (2000), 87-94.
4. Wang, C.C. and Chen, C.K., "Three-dimensional inverse heat transfer analysis during the grinding process", ***Proc. IMechE, Part C: J. Mechanical Engineering Science***, Vol. 216, (2002), 199–212.
5. Hebi, Y. and Man, Y., "Inverse problem-based analysis on non-uniform profiles of thermal resistance between strand and mould for continuous round billets casting", ***J. Mater. Process. Technol.*** Vol. 183, (2007), 49–56.
6. Beck, J.V., Blackwell, B. and Clair, C.R.St., "Inverse

Heat Conduction: Ill-Posed Problems", ***John Wiley and Sons***, New York, (1985).
7. Zhou, Jianhua, Zhang, Yuwen, Chen, J.K. and Feng, Z.C., " Inverse estimation of spatially and temporally varying heating boundary conditions of a two-dimensional object", ***International Journal of Thermal science***, Vol. 49, (2010), 1669–1679
8. Tikhonov, A.N. and Arsenin, V.Y., "Solution of Ill-Posed Problem", ***Winston and Sons***, Washington, DC (1977).
9. Ozisik, M.N. and Orlande, H.R.B., "Inverse heat transfer fundamentals and applications", ***Taylor and Francis***, New York (2000).
10. Ranjbar, A.A. and Mirsadeghi, M., "An Inverse Estimation of Initial Temperature Profile in a Polymer Process", J***. Polym. Eng. Sci.***, Vol. 48, (2007), 133-140.
11. Pourshaghaghy, A., Kowsary, F. and Behbahaninia, A., "Comparison of Four Different Versions of the Variable Metric Method for Solving Inverse Heat Conduction Problems", ***Int. J. Heat Mass Transfer***, Vol. 43, (2007), 3.
12. Leea, K.H., Baeka, S.W. and Kimb, K.W., "Inverse radiation analysis using repulsive particle swarm optimization algorithm". ***Int. J. Heat Mass Transfer***, Vol. 51(11-12), (2008), 2772-2783.
13. Famouri, M., "Inverse estimation of heat transfer coefficient at the metal-mould interface in the two dimensional solidification with temperature dependent thermo-physical properties", M.S. Thesis, University of Mazandaran, (2008).
14. Ranjbar, A.A., Famouri, M. and Imani, A., " A Transient Inverse Problem in Simultaneous Estimation of TDTP Based on MEGA", ***Inter. J. Numer. Methods Heat Fluid Flow***, Vol. 20 (2), (2010), 201-217.
15. Imani, A., Ranjbar, A.A. and Esmkhani, M., "Simultaneous estimation of temperature-dependent thermal conductivity and heat capacity based on modified genetic algorithm". ***Inverse Probl. Sci. Eng***., Vol. 14(7), (2006), 767-783.
16. Garcia, S., "Experimental design optimization and thermophysical parameter estimation of composite materials using genetic algorithms", PhD thesis, Virginia Polytechnic Institute and State University, USA, (1999).
17. Imani, A., " Simultaneous estimation of temperature dependent thermal conductivity and heat capacity using Inverse Heat Conduction Problem (IHCP) based on genetic algorithm", M.S. Thesis, University of Mazandaran, (2005).
18. Ranjbar, A.A., Ezzati, M. and Famouri, M., "Optimization of Experimental Design for an Inverse Estimation of the Metal-Mold Heat Transfer Coefficient in the Solidification of Sn–10% Pb", ***J. Mater. Process. Technol***., Vol. 209, 15-16, (2009), 5611-5617.
19. Arunkumar, S., Sreenivas Rao, K.V. and Prasanna Kumar, T.S., "Spatial variation of heat flux at the metal–mold interface due to mold filling effects in gravity die-casting", ***Int. J. Heat Mass Transfer***, Vol. 51 (11), (2008), 2676–2685.
20. Franklin, J.R. and Das, A.A.," Squeeze casting : a review of the status", ***Brit. Foundryman***, March, (1983), 150–158.
21. Chadwick, G.A. and Yue, T.M., "Principles and applications of squeeze casting", ***Met. Mater***. Vol. 5(1), (1989), 6–12.
22. Morton, J.R. and Barlow, J., "Squeeze casting: from a theory to profit and future", ***J. Inst. Brit. Foundryman***, Part 1 Vol. 87, (1994), 23–28.
23. Loulou, T., Artyukin, E.A. and Bardon, J.P., "Estimation of thermal contact resistance during the first stage of metal solidification process: I-experiment principle and modification", ***Int. J. Heat Mass Transfer***, Vol. 42, (1999), 2119–2127.
24. Lau, F., Lee, W.B., Xiong, S.M. and Liu, B.C., "A study of the interfacial heat transfer between an iron casting and a metallic mold***", J. Mater. Process. Technol***. Vol. 79, (1998), 25-29.
25. Martorano, M.A. and Capocchi, J.D.T., "Heat transfer coefficient at the metal-mould interface in the unidirectional solidification of Cu-8% Sn alloys", ***Int. J. Heat Mass Transfer***, Vol. 43, (2000), 2541–2552.
26. Adili,A., Hasni, N., Kerkeni, C. and S. Ben Nasrallah, "An inverse problem based on genetic algorithm to estimate thermophysical properties of fouling", ***International Journal of Thermal Science***, Vol. 44 (2005) 1090–1097.
27. Santos, C.A., Siqueira, C.A., Garcia, A., Quaresma, J.M.V. and Spim, J.A., "Metal-mold heat transfer coefficients during horizontal and vertical unsteady solidification of Al–Cu and Sn–Pb alloys", ***Inverse Problem in Science and Engineering***, Vol. 12, (2004), 279–296.
28. Aweda, J.O. and Adeyemi, M.B., "Experimental determination of heat transfer coefficient during squeeze casting of aluminium", ***J. Mater. Process. Technol***. Vol. 209, (2009), 1477–1483.
29. Cho, I.S. and Hong, C.P., "Evaluation of heat-transfer coefficients at the casting/die interface in squeeze casting", ***Int. J. Cast Metals Res***. Vol. 9, (1996), 227–232.
30. Shamsundar, N., Rooz, E., Minkowycz, W.J., Sparrow, E.M., Schneider, G.E. and Pletcher, R.H., "Handbook of Numerical Heat Transfer, first edition", John Wiley and Sons, New York, (1988), 747–786.
31. Garcia, A., Ferreira, I.L., Spinelli, J.E. and Pires, J.C., "The effect of melt temperature profile on the transient metal/mold heat transfer coefficient during solidification", **J. Mater. Sci. Eng**, (2005), 317–325.
32. Santos, C.A., Quaresma, J.M.V. and Garcia, A., " Determination of transient interfacial heat transfer coefficient in chill mold castings", ***J. Alloys Compd***., Vol. 319, (2001), 174-186.
33. Beck, J.V. and Arnold, K.J., "Parameter Estimation in Engineering and Science", Wiley, New York, (1977).
34. Goldberg, D.E., "Genetic Algorithms in Search Optimization and Machine Learning", MA: Addison-Wesley, (1989).
35. Michalewicz, Z., "Genetic Algorithms+Data Structure=Evolution Program", Berlin: Springer, (1996).
36. Davis, L., "Handbook of Genetic Algorithms", New York: Van Nostrand Reinhold, (1991).